NUCL SCI TECH (2019) 30:7
https://doi.org/10.1007/s41365-018-0531-9

Room-temperature test system for 162.5 MHz high-power couplers

Long Chen[1,2] · Shen-Hu Zhang[2] · Yong-Ming Li[2] · Ruo-Xu Wang[2] · Tiancai Jiang[2] · Lei Yang[1,2] · Chun-Long Li[2] · An-Dong Wu[2] · Shi-Chun Huang[2] · Feng Pan[1,2] · Xin-Meng Liu[1,2] · Yuan He[2]

Received: 1 December 2017 / Revised: 13 June 2018 / Accepted: 16 June 2018 / Published online: 2 January 2019

Abstract Fundamental power couplers are crucial components for feeding radio frequency power to accelerating cavities. Couplers must be tested and conditioned on a room-temperature test stand to evaluate and potentially improve their performance before being installed in an accelerating cavity. A new test system has been designed and is under construction at the institute of modern physics. For this test system, multiple conditioning modes, including the pulse mode, CW mode, and amplitude-sweeping mode, have been embedded in the low-level radio frequency system of the test stand. All of these conditioning modes can be run manually or automatically. In addition, a novel test cavity is proposed and has been designed, which facilitates non-contact conditioning and a multi-purpose test stand.

Keywords Couplers conditioning · Test stand · LLRF control system · Test cavity

This work was supported by the National Key Basic Research Program of China (973 Program) (No. 2014CB845504).

✉ Long Chen
chenlong15@impcas.ac.cn

Shen-Hu Zhang
zhangsh@impcas.ac.cn

Yong-Ming Li
ymli@impcas.ac.cn

1 University of Chinese Academy of Sciences, Beijing 100049, China

2 Institute of Modern Physics, Chinese Academy of Sciences, Lanzhou 730000, China

1 Introduction

162.5 MHz HWR010 and HWR015 superconducting cavities (SSCs) have been used in the Chinese ADS 25 MeV demo SRF Linac [1–3]. Each cavity is fed with RF power by one-input high-power coupler [4, 5]. The maximum power of the coupler design is 20 kW in the traveling mode. Prior to assembly, couplers need to be tested and conditioned at room temperature. In addition, the characteristics of the conditioning phenomenon can also be thoroughly investigated during the conditioning process [6–9].

The previous test system for couplers at IMP consists of an RF power system, an LLRF control system, a test stand, and auxiliary devices. Figure 1 shows a block diagram of the previous test system. In the process of conditioning, the source RF signal of 162.5 MHz is modulated depending on the state of the test stand or the needs of the conditioning modes. The modulated signal is then amplified by a solid amplifier to produce RF power, which travels through the couplers and is absorbed by a load in the traveling wave conditioning mode. In the standing wave conditioning mode, the load is replaced with a short-circuit plate.

There are several problems associated with the previous test system. On the one hand, the LLRF control device and the interlock system are not ideal due to the following disadvantages:

(a) Although the previous test system can be run in auto-mode, this does not apply to amplitude-sweeping mode. In addition, automatic reset is not available, when interlock protection occurs.
(b) The interlock system is not fast enough. The response time of the arc/vacuum interlock is

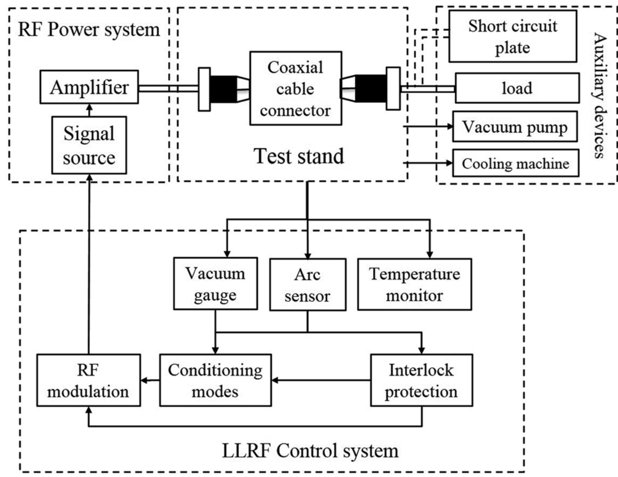

Fig. 1 Block diagram of the previous test stand system

20 μs/2 ms for the previous system. 2 μs/1 ms is the basic requirement for the new system.

(c) The output RF source signal is not precise in amplitude-sweeping mode. The output RF source signal might overshoot when the RF amplitude is swept in a period of less than 0.1s.

In addition, several problems have been discovered from operation with the test stand:

(a) The antenna tips (Fig. 2a) is not conditioned. The antenna tips are replaced with inner connectors when the couplers are mounted on the test stand as shown in Fig. 2b.

(b) Dust particles might be created or spread when the antenna tips are installed prior to installing the conditioned couplers to the SSCs.

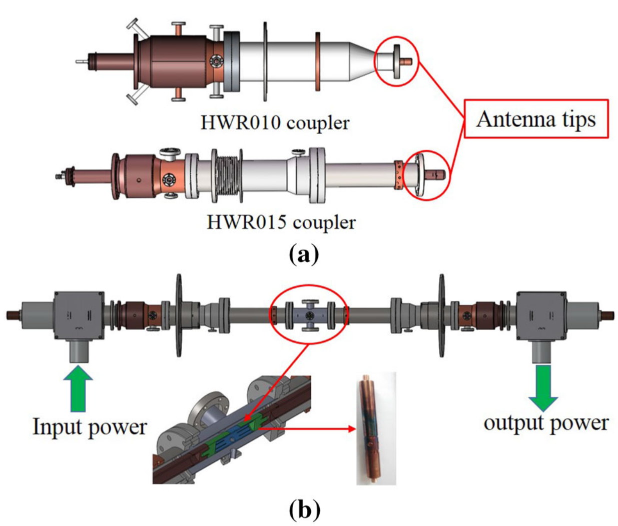

Fig. 2 (Color online) **a** HWR010 coupler and HWR015 coupler; **b** a pair of couplers assembled with a coaxial connector

(c) In practice, it is not easy to connect the inner conductors of the couplers with coaxial connectors. The connectors are often burned by heat deposition due to a loose connection.

As a result, the development of a new test system is necessary and urgent. The LLRF system was redeveloped completely to address the issues regarding the LLRF control system. A test cavity was designed to replace the previous coaxial connector for the test stand in an attempt to solve the problems caused by the contacting conditioning method. This work is a thorough introduction of the new LLRF control system and the design of the test cavity.

2 Development of LLRF control system

The functions of the new LLRF control system can be classified into data sampling, RF modulation, interlock protection, and conditioning modes achievement. All of these functions are integrated based on a development board. When we chose the board, the following requirements were considered:

(a) Considering the basic needs and future update, 6 analog input (AI) channels, 4 analog output (AO) channels and 15 digital I/O (DI/O) channels are required.

(b) Both the maximum AI sampling rate and the maximum AO update rate must be faster than 100 KS/s.

(c) The minimum pulse width for the DI/O channel should be less than 100 ns.

Taking all these requirements into account, the Myrio-1900 [10] was chosen as the core of the LLRF control system. The Myrio-1900 is a mature commercial development board with 10 AI, 6 AO and 40 DI/O Channels in total. It has an FPGA and a double-core ARM processor. The maximum AI sampling rate and maximum AO update rate achieved was 200 KS/s and 300 KS/s, respectively. The minimum pulse width for the DI/O is 20 ns. Therefore, myrio-1900 board is powerful enough for the proposed development. The entire system was developed using LabVIEW2016 software. Figure 3 shows the LabVIEW control system interface on the host PC.

2.1 RF modulation

For the LLRF control system, the RF source often needs to be turned on or off swiftly. For example, RF pulse generation requires turning the RF source on and off at a certain frequency and interlocks are required to cut off the RF source as fast as possible. ZYSWA-2-50DR RF

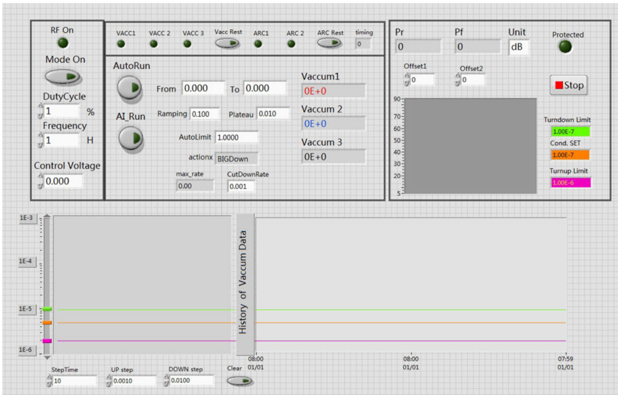

Fig. 3 (Color online) Control system interface

switch [11] was selected to fulfill these tasks. It has a fast rise (6 ns) and is highly reliable.

On the other hand, it is necessary to adjust the RF power either manually or automatically (as in the amplitude-sweeping mode or the auto-conditioning mode. We achieve this requirement by modulating the RF source with a voltage variable attenuator (VVA). The VVA should be reliable and resilient and have a short rise/fall time. The ZX73-2500+ [11] was chosen to accomplish this task. It has a rise/fall time of 14 μs/25 μs and is resilient to workplace temperature and to the input control voltage and input RF power. The control voltage range from 1.4 to 4.6 V (corresponding to an attenuation range of 10–35 dB) was chosen because of the excellent output stability.

2.2 Interlock system

The interlock system guarantees the safety of the coupler conditioning. Basically, the interlock system comprises an arc interlock and a vacuum interlock. When arc events occur in the couplers, energy deposits on the inner copper surface or the ceramic windows. If such processes last for a long period of time, the couplers might be permanently damaged [12]. The vacuum in the couplers should be restricted to less than a certain threshold value (generally 10^{-3} Pa in this case). When the pressure in the couplers reaches a certain level, plasma might be created. In that case, the metal on the inner surface of the couplers might sputter out due to the bombardment of the plasma. This causes the performance of the couplers to degrade [12]. Therefore, both interlocks are mandatory. The overall interlock feedback is described in Fig. 4. To improve the response time and reliability, the interlock programs were written in FPGA. Once the arc detectors identify an arc event, digital interlock signals are sent to the control system, and the RF switch is swiftly turned off.

The response times of the arc interlock and vacuum interlock were measured separately. The lower waveforms are both the source RF signals to drive the solid amplifier as shown in Fig. 5. In Fig. 5a, the upper line is the arc protection digital signal from the arc detector. In Fig. 5b, the upper line is the given vacuum analog signal, which exceeds the vacuum protection threshold. The measured delayed times (response times) for the arc and vacuum interlocks are 440 ns and 232 μs, respectively. These values are both one order of magnitude smaller than the response times of the arc detector and vacuum gauge.

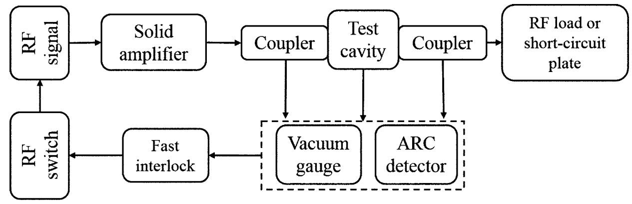

Fig. 4 Overall interlock loop

2.3 Conditioning mode

2.3.1 *Pulse/CW mode*

Practical operating experience both at IMP and other laboratories have shown that the conditioning of the couplers in pulse mode are the most demanding step of the entire progress [13]. This is primarily because outgassing caused by multipacting (MP) [14–16] is initially severe. Pulse mode in the low duty factor can make conditioning sustainable, but slower, to avoid serious outgassing by reducing the duration of MP in the couplers. With the advance of conditioning, the duty factor will be turned up and eventually it moves on to the CW mode as this factor becomes 100%. We make use of the RF switch to produce pulses of adjustable length by turning the signal on and off. The pulse length can be calculated using a PC through the input repetition frequency and duty factor. Based on this value, the FPGA controls the duration of the driving TTL signal. Because of the excellent timing of the FPGA, RF pulses even shorter than 1 μs can be generated.

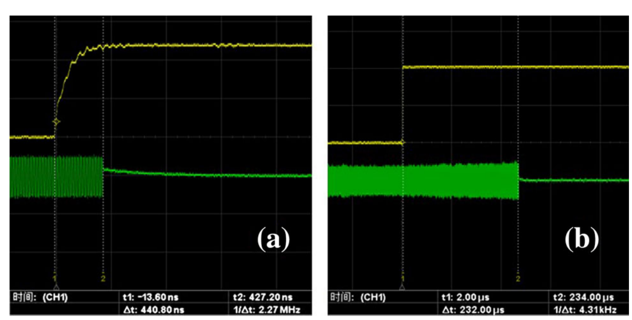

Fig. 5 (Color online) Measurement results of the response time of the interlock system

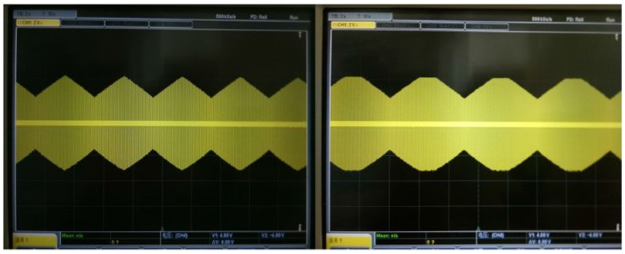

Fig. 6 (Color online) RF power signal picked up from directional couplers in triangle amplitude-sweeping mode and trapezoid amplitude-sweeping mode

2.3.2 Amplitude-sweeping mode

Sweeping the amplitude of the RF power is an important way to condition couplers because of the possible recurrence of MP at certain RF power points. Combined with extremely short RF pulses, the amplitude-sweeping mode is very effective particularly in the initial conditioning stage. The previous system was only able to provide triangle-wave amplitude sweeping. However, due to the impreciseness of timing in PC, amplitude sweeping cannot be perfectly controlled. As a result, the driving voltage may exceed the upper limit, especially when the ramping time of the driving voltage is set too short (approximately 100 ms). RF amplitude modulation has been achieved as outlined. With regard to the problem of the output voltage overshooting, we have addressed this problem by coding portions of the amplitude-sweeping program in FPGA. The ramping time of the driving voltage can be adjusted in the range of 1 ms to ∞ for the new system. In order to improve the efficiency of conditioning, we made it possible to sweep RF amplitude with a trapezoid wave envelope. Figure 6 represents the program test results with a source signal at a frequency of 162.5 MHz. The repetition frequency and duty cycle of the pulse are 100 Hz and 1%, respectively.

2.3.3 Auto-running strategy

To accelerate the condition and test progress, an auto-running program was developed for the control system. All conditioning modes can be shifted to the auto-mode. One of the goals of conditioning is degassing the inner surface of the couplers. The principle is to keep outgassing continuous but moderate. Figure 7 shows the block diagram of the feedback loop of the auto-conditioning mode. In the program for the auto-conditioning mode, the vacuum data and its increasing rate are both regarded as factors that decide what action the system should take. In the non-sweeping mode, the target of the modulation is the driving voltage of the VVA attenuator. In the sweeping mode, the target of the modulation is the upper sweeping limit.

The detailed flow chart of the strategy of automatic conditioning is shown in the right diagram of Fig. 7. There are four thresholds; limit1, limit2, and limit3 set the vacuum and limit4 sets the rate of increase of the vacuum. Initially, the vacuum is below limit1 and changes with RF power due to MP. When the vacuum is lower than limit1, the target will be increased until the vacuum is higher than limit2 and lower than limit3. However, when the vacuum exceeds limit3, the target will be continuously reduced until the vacuum is less than limit2. Simultaneously, the rate of increase of the vacuum is monitored. Once this rate exceeds limit4, a drastic reduction will be made to the target. In the non-sweeping mode, the system simply compares the maximum vacuum value and maximum vacuum increasing rate of all vacuums with the thresholds. In the sweeping mode, the vacuums will fluctuate

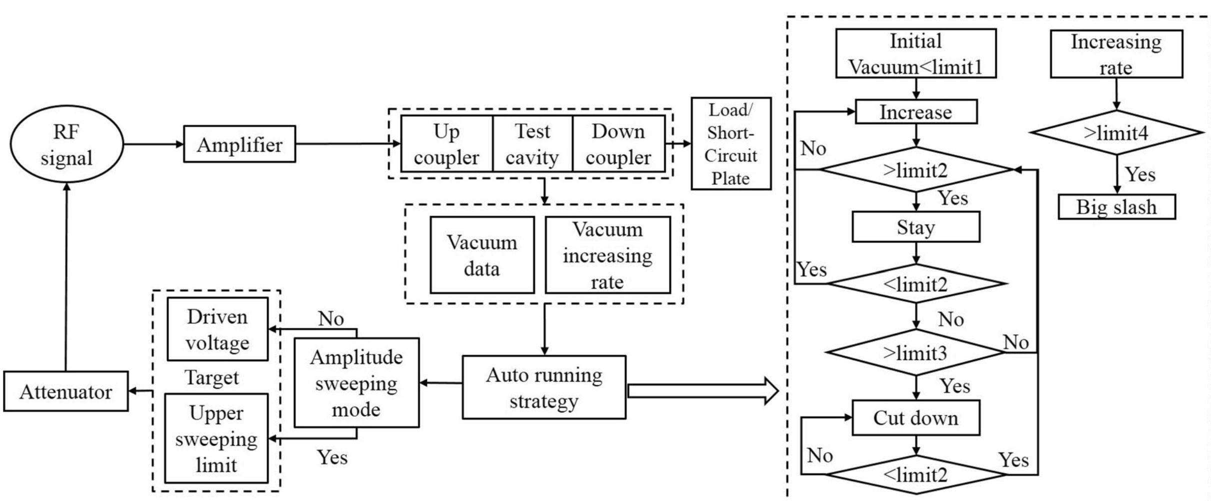

Fig. 7 Block diagram of the logic loop of the auto-conditioning mode and the auto-running strategy

significantly. In that case, the maximum peak vacuum value and the maximum peak increasing rate over a duration of 10 seconds are recorded and compared with the thresholds. It is worth noting that auto rest after interlock protection is available for the new system, which is a big step toward completely automatic conditioning.

3 Design of test box

3.1 Design principles

As mentioned in the introduction, we proposed to use cavity structure instead of coaxial structure to match a pair of couplers. The following principles for designing the test cavity were implemented:

(a) Small size is desired because of the reduced cost of materials and realization for baking.
(b) The antenna tips of the couplers must not form mechanical contact with other parts. This is the key point that solves the problems associated with the previous test stand.
(c) The power dissipated on the cavity should be less than 300 W with 20 kW forward power to avoid extra cooling design.
(d) RF passband (3 dB for S21) should be at least wider than 5 MHz. A wider passband produces a better detuning tolerance for the cavity.

3.2 Analysis of power loss in test cavity

In order to fulfill the requirement of principle(c), it is mandatory to analyze the exact power loss in the test cavity. The power transmission for the conditioning situation with the test cavity can be described with a model of a two-port network, whose equivalent circuit is shown in Fig. 8. The test cavity is simplified to an RLC parallel circuit. The coupling of the upstream coupler and the downstream couplers are β_1 and β_2, respectively. The reflection coefficient can be expressed as [17]

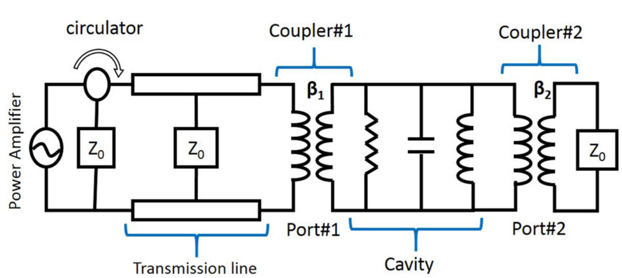

Fig. 8 The equivalent circuit of two-port cavity model

$$\Gamma = \frac{\beta_1 - \beta_2 - 1}{1 + \beta_1 + \beta_2}. \tag{1}$$

As a result, the reflected power (P_{re}) can be obtained [18]:

$$Pre = \Gamma^2 Pf = \left(\frac{\beta_1 - \beta_2 - 1}{1 + \beta_1 + \beta_2}\right)^2 Pf. \tag{2}$$

For the entire test stand, there is such a relation for the forward power (Pf), the reflection coefficient, the transmitted power from port2 (Pt) and the power loss in the cavity (Pc):

$$1 = \Gamma^2 + \frac{Pc}{Pf} + \frac{Pt}{Pf}, \tag{3}$$

where Pt is equal to the power dissipated from port 2, so Pt can also be replaced with $\beta_2 Pc$. Substituting $\beta_2 Pc$ for P_t in Eq. (2) gives rise to the expression Pc as a function of Pf, β_1 and β_2.

$$Pc = \frac{4Pf\beta_1}{(1 + \beta_1 + \beta_2)^2} \tag{4}$$

For the purpose of simplifying the structure of the test cavity, β_1 and β_2 are set to be the same. Then, the expressions Pc and Pre are transformed into:

$$Pc = \frac{4Pf\beta}{(1 + 2\beta)^2}, \tag{5}$$

$$Pre = \frac{Pf}{(1 + 2\beta)^2}. \tag{6}$$

And Pt can be derived by using $Pt = \beta_2 Pc$:

$$Pt = \frac{4\beta^2 Pf}{(1 + 2\beta)^2}. \tag{7}$$

The power design capability of the couplers is 20 kW. Therefore, Pf is set as 20 kW. The lines in Fig. 9 exhibits the change of the power loss, reflected power and the transmitted power from port2 with varying coupling at $Pf = 20$ kW. The dots in Fig. 9 are the simulated results

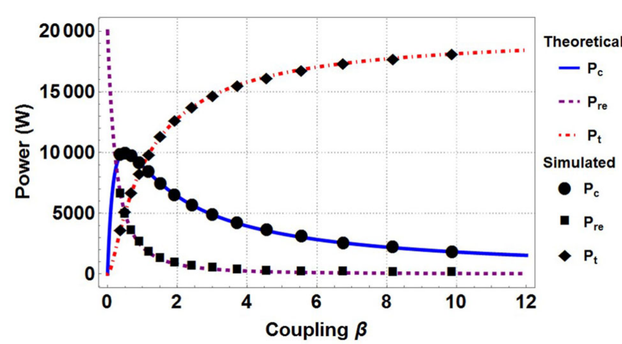

Fig. 9 (Color online) Theoretical and simulated results of Pc, Pre, Pt, with 20 kW forward power

using the frequency domain solver and the eigen solver of CST [19]. Apparently, the simulated results are close to the theoretical line, which validates the previous induced equations.

It is readily observed that the reflected power decreases rapidly with an increase in coupling, and the power loss reaches its peak at 0.5 and decreases as the coupling is continuously increased. Further calculations indicate that as long as the coupling is large than 22, the reflected power is less than 10 W, which can be neglected. As previously indicated, the power loss on the test cavity should be less than 300 W when Pf reaches 20 kW. Using Eq. (3) to perform calculations to ensure that the requirement for power loss restriction is satisfied, we determined that the coupling should be larger than 66.

3.3 Design of structure and electromagnetic optimization

Because of principle (a), a QWR (quarter-wave resonator)-like cavity was used for optimization [20]. In order to make the assembly of the test stand more compact, the coupling ports are placed on the same side. According to the analysis in the previous section, the coupling of the ports for the cavity should be no less than 66. However, it is impossible to achieve such a high coupling with a common structure unless we replace the antenna tips of the couplers with larger ones. However, this idea conflicts with principle (b). Instead, we added tubes to the inner conductor, in which the antenna tips of the couplers can fit as shown in image (a) of Fig. 10. The final cavity design is shown in image (b) of Fig. 10. It is worth noting that both types of ports for the HWR010 couplers and the HWR105 couplers have been preserved. Tuners can then be installed on the rest of the ports when a pair of ports are used to condition the couplers so as to ensure that the center frequency of the passband is 162.5 MHz.

A four-port test cavity has been optimized with CST for both cases (with couplers HWR010 and couplers HWR015 mounted). Copper was chosen as the material of the cavity. In the process of optimization, the cavity size, assembling space, passbands, field distributions, coupling, and power loss have been taken into account. Figures 11 and 12 show the S-parameter curves and the field distributions for both cases. The electromagnetic parameters of interest are summarized in Table 1.

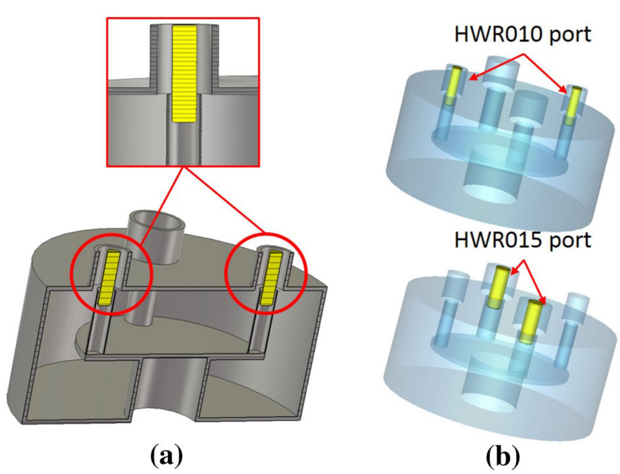

Fig. 10 (Color online) Design of structure of test cavity

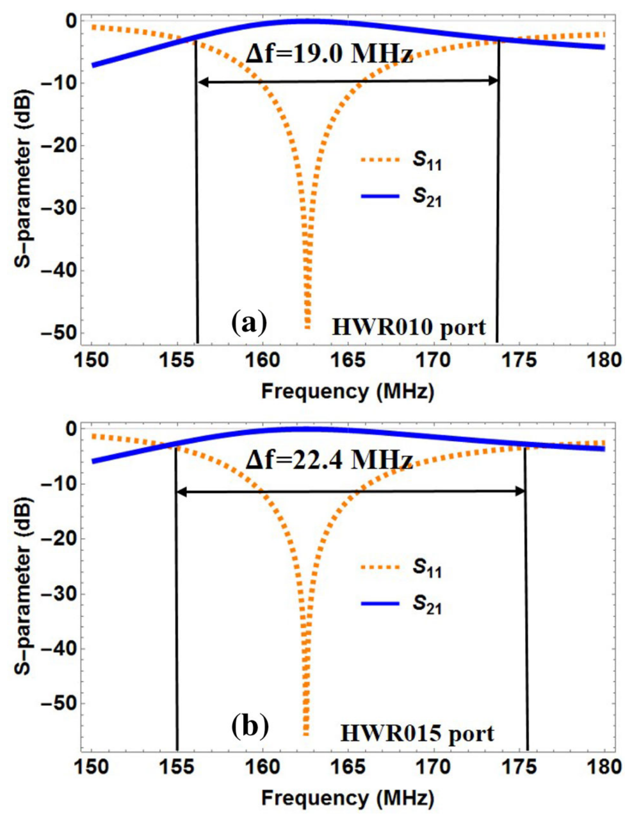

Fig. 11 (Color online) S-parameter curves of test cavity

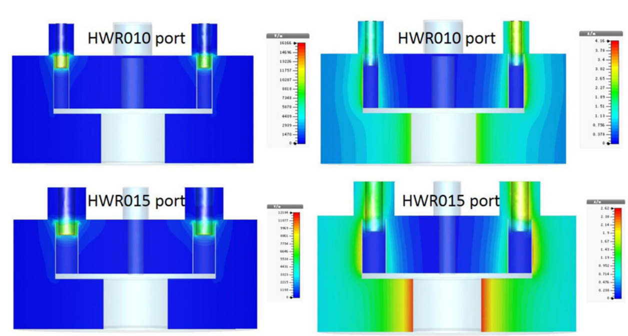

Fig. 12 (Color online) Electromagnetic fields distributions of test cavity

Table 1 Electromagnetic parameters of the optimized test cavity

Parameter	Port type 1	Port type 2
β	496.7	583.2
Epeak@20 kW (MV/m)	2.3	1.7
Pc@20 kW (W)	40	34
Pre@20 kW (W)	0.02	0.014
Band width @-3 dB (MHz)	19.0	22.4

4 Summary

The development of an LLRF control system for high-power coupler test stands has been completed. Multiple conditioning modes and fast interlocks have been realized. The control system has been implemented for several months. A multi-purpose test cavity has been designed and optimized, which hopefully will facilitate non-contact conditioning. The test cavity is under construction, and the test stand will be put into operation in the near future.

References

1. W.L. Zhan, H.S. Xu, Advanced fission energy program–ADS transmutation system. Bull. Chin. Acad. Sci. **27**, 375 (2015). https://doi.org/10.3969/j.issn.1000-3045.2012.03.017
2. L.J. Wen, S.H. Zhang, Y.M. Li et al., Study of medium beta elliptical cavities for CADS. Chin. Phys. C **40**, 027004 (2016). https://doi.org/10.1088/1674-1137/40/2/027004
3. A.D. Wu, S.H. Zhang, W.M. Yue et al., Design study on medium beta superconducting half-wave resonator at IMP. Nucl. Sci. Tech. **27**, 80 (2016). https://doi.org/10.1007/s41365-016-0081-y
4. T.M. Huang, W.M. Pan, Q. Ma et al., High power input coupler development for BEPCII 500 MHz superconducting cavity. Nucl. Instrum. Methods Phys. Res. A **623**, 895 (2010). https://doi.org/10.1016/j.nima.2010.08.108
5. Y.G. Martínez, M. Baylac, P. Boge et al., Final results of power conditioning of SPIRAL 2 couplers. Nucl. Instrum. Methods Phys. Res. A **870**, 37 (2017). https://doi.org/10.1016/j.nima.2017.07.004
6. W.M. Pan, T.M. Huang, Q. Ma et al., Development of a 500 MHz high power RF test stand. Chin. Phys. C **36**, 355 (2012). https://doi.org/10.1088/1674-1137/36/4/011
7. S. Kazakov, B.M. Hanna, T.N. Khabiboulline et al., Test stand for 325 MHz power couplers. Paper presnented at Proceedings of LINAC2014, Geneva, Switzerland, August 31–5 September (2014)
8. H. Jenhani, T. Garvey, A. Variola, RF conditioning studies of input power couplers for superconducting cavities operating in pulsed mode. Nucl. Instrum. Methods Phys. Res. A **595**, 549 (2008). https://doi.org/10.1016/j.nima.2008.07.111
9. R. Kumar, M. Jose, G.N. Singh et al., RF characterization and testing of ridge waveguide transitions for RF power couplers. Nucl. Instrum. Methods Phys. Res. A **838**, 66 (2016). https://doi.org/10.1016/j.nima.2016.07.029
10. User guide and specifications, NI myRIO-1900. http://www.ni.com. Accessed 20 Sept 2017
11. Minicircuits, Hompage. https://www.minicircuits.com. Accessed 20 Sept 2017
12. H. Padamsee, *RF Superconditivity: Science, Technology, and Applications* (Wiley-VCH, Berlin, 2009), p. 292
13. Y. Yamamoto, T. Honma, E. Kako et al., High gradient cavity performance for the ILC KEK. in STF-2 cryomodule. Paper presented at *Proceedings of LINAC2016*,Busan, Korea, 8-13 May 2016. http://accelconf.web.cern.ch/AccelConf/ipac2016/doi/JACoW-IPAC2016-WEPMB017.html. https://doi.org/10.18429/JACoW-IPAC2016-WEPMB017
14. R. Parodi, Multipacting. Paper presented at *Proceedings, CAS - CERN Accelerator School: RF for Accelerators*, Ebeltoft, Denmark, 8–17 (2010). http://cds.cern.ch/record/1406274. https://doi.org/10.5170/CERN-2011-007.447
15. C. Wang, L.H. Chang, M.H. Chang et al., Mitigation of multipacting, enhanced by gas condensation on the high power input coupler of a superconducting RF module, by comprehensive warm aging. Nucl. Instrum. Methods Phys. Res. A **872**, 150 (2017). https://doi.org/10.1016/j.nima.2017.08.012
16. P.N. Ostroumov, S. Kazakovb, D. Morrisa et al., Suppression of multipacting in high power RF couplers operating with superconducting cavities. Nucl. Instrum. Methods Phys. Res. A **856**, 77 (2017). https://doi.org/10.1016/j.nima.2017.02.081
17. T.P. Wangler, *RF Linear Accelerators*, 2nd edn. (Wiley-VCH, Berlin, 2008), p. 145
18. D.M. Pozar, *Microwave Engineering*, 4th edn. (Wiley, Hoboken, 2005), p. 82
19. Computer Science Technology, Hompage. https://www.cst.com. Accessed 20 Dec 2017
20. K. Zhou, L. Yang, G.P. Sun et al., Geometry dependent multipacting of a superconducting quarter-wave resonator at PKU. Chin. Phys. C **37**, 077002 (2013). https://doi.org/10.1088/1674-1137/37/7/077002